

## Characterization of Microstructure and Magnetic Properties of $\text{CaCu}_3\text{Mn}_4\text{O}_{12}$ by Sol Gel Route

A. R. M. Warikh<sup>1</sup>, A. Nurulhuda<sup>1</sup> and A. R. Jefferie<sup>1</sup>

<sup>1</sup>*Department of Engineering Materials, Faculty of Manufacturing Engineering,  
Universiti Teknikal Malaysia Melaka, Hang Tuah Jaya,  
76100 Durian Tunggal, Melaka, MALAYSIA*

The crystallization of single phase  $\text{CaCu}_3\text{Mn}_4\text{O}_{12}$  (CCMO) was successfully synthesized via sol gel method and was fairly well densified at relative low temperature under atmospheric condition. The microstructure characteristic, phase formation and magnetic properties of  $\text{CaCu}_3\text{Mn}_4\text{O}_{12}$  ceramics were investigated and characterized by XRD, FESEM and VSM testing. It was found that the pure phase with highly crystalline of  $\text{CaCu}_3\text{Mn}_4\text{O}_{12}$  were formed after sintered at 700°C under atmospheric condition as support by XRD analysis. FESEM result shows the significant influence of sintering parameter on the microstructure behavior of  $\text{CaCu}_3\text{Mn}_4\text{O}_{12}$ . The smaller particle size with higher grain boundary and less of porosity were found for the sample sintered at 700°C to 800°C. The samples show the 'superparamagnetism' behavior where the M-H curves are linear with the field and have a smaller value of coercivity at room temperature. Sintering at 800°C produced the sample with lowest Hc value due to the phenomenon over grown of magnetocrystallites, grain size and grain boundaries.

### INTRODUCTION

Calcium cuprum manganese oxide ( $\text{CaCu}_3\text{Mn}_4\text{O}_{12}$ ) has been considerable interest because of their high magnetoresistive property. In the previous paper [1] the finding of colossal magneto resistance effect of CCMO was reported by Li et al., (2005). The good magnetoresistance properties of CCMO ceramic was reported at 20K and 5 tesla due to the special of double distorted of perovskite-like phase structure that have possessed colossal magnetoresistance in a wide range temperature [2].

For the synthesis of perovskite-type oxides, the sol gel routes have been proved to be very useful, obtaining well crystallized powder and excellent stoichiometric control [3]. Sol gel routes also give higher composition and microstructure at relative low sintering temperature. This method is based on the principle that the reactant are mixed in the molecular level where the low calcinations

temperature is needed to produce fine powders with high purity [4]. From this point of view, the availability of good sinterability powder, with homogeneous microstructure, smaller grain size and good crystallinity is desirable to produce a pure phase with highly crystalline of  $\text{CaCu}_3\text{Mn}_4\text{O}_{12}$ .

To the best of our knowledge, the CCMO ceramic reported up to now obtained by the combination of sol gel process with high oxygen sintering pressure at 700°C for 3 days under 0.18kbar (2600Psi) [5]. According to the previous literature, we are proposed and prepared the CCMO synthesis via sol gel under atmospheric pressuring condition with the lowest optimum sintering temperature and dwelling time.

In our recent work, we have prepared a simple powder preparation method by using the citric acid to chelate the metal ions, while ethylene glycols react as solvent for the

<sup>1</sup>Corresponding author. Tel: + 6(06)3316420; Fax: + 6(06)331 6411/6431  
E-mail: warikh@utem.edu.my

polymerization between citric acid and ethylene glycol. In addition, the present paper also has been attempted to verify the applicability of atmospheric sintering condition for producing higher purity with a good properties of CCMO via sol-gel synthesis at optimum processing parameter.

### EXPERIMENTAL PROCEDURE

The CCMO ceramics have been prepared by sol gel route. The starting materials used were calcium carbonate ( $\text{CaCO}_3$ ), copper oxide ( $\text{CuO}$ ), manganese nitrate tetrahydrate ( $\text{Mn}(\text{NO}_3)_2 \cdot 4\text{H}_2\text{O}$ ) were weight accurately and dissolved in a citric acid ( $\text{C}_6\text{H}_8\text{O}_7$ ), nitric acid ( $\text{HNO}_3$ ) and ethylene glycol ( $\text{HOCH}_2\text{CH}_2\text{OH}$ ). The stoichiometric amount of  $\text{CuO}$  and  $\text{CaCO}_3$  in 0.6M citric acid (CA) with molar ratio of [citrates/metallic ion] is 1:2 by simple stirring at room temperature and then heat slowly up to  $90^\circ\text{C}$  for 6h in order to remove the excess water, at the end of which a clear light blue and sticky gel of solution. The light blue and sticky gels formed were treated in oven at  $140^\circ\text{C}$  for 18h to fully evaporate and promote polymerization. The powder was ground in agate mortar, pressed into a disc at 2.9 ton (369 MPa) for 10s under Uniaxially Hydraulic Pressing Machine and calcined at  $500^\circ\text{C}$  and  $600^\circ\text{C}$  for 12h. Pellets then were well densified at relative low temperature ( $600$ ,  $700$  and  $800^\circ\text{C}$ ) in high temperature furnace under atmospheric condition for 18, 24, 36 and 72h.

The phases of samples were checked by X-ray diffraction using Cu-K $\alpha$  radiation at range  $10^\circ \leq 2\theta \leq 90^\circ$  at minimum step interval of  $0.001^\circ$ . The morphology of samples was obtained using field-emission scanning electron microscope (FESEM) and the magnetization data were carried out with DMS vibrating sample magnetometer (VSM) for maximum magnetic field 25 KOe at room temperature. The parameter like specific saturation magnetization ( $M_s$ ), coercive force ( $H_c$ ) and remanence ( $M_r$ ) were deduced.

### RESULT AND DISCUSSION

#### Phase Analysis of CCMO Ceramic by X-ray Diffraction

The CCMO phase evolution was monitored by X-ray analysis. The best condition of sintering parameter to obtain the single phase of CCMO was evaluated. All the peak positions were identifying by comparison with CCMO JCPDS file No. 01-072-0401. At  $600^\circ\text{C}$ , only board peaks of CCMO appeared with the certain trace elements of  $\text{CuO}$  (ICSD: 44-0706). However, the secondary phase of  $\text{Mn}_2\text{O}_3$  (ICDD: 01-072-0401) exists at this temperature and it can be observed until the sintering temperature increased to  $700^\circ\text{C}$ .

The sintered samples at  $700^\circ\text{C}$  for 18h showed the main peaks related to the pure CCMO system compared to the peaks resulted from  $600^\circ\text{C}$  where the diffraction peaks become progressively narrow, attributed to the increasing crystallite size and grain growth [6]. Based on the Fig. 1, the formation of CCMO peaks enhance by the reduction significant of  $\text{CuO}$  peaks when sintered up to  $700^\circ\text{C}$ ; suggesting that the optimum lowest temperature ( $\sim 700^\circ\text{C}$ ) is needed for complexion of the reaction during sintering process. It was an evident that the increasing sintering temperature also caused a relative strength of the diffraction peaks due to the effect and beneficial of crystal growth. There are also only significant differences between phase formation of the sample sintered between  $700^\circ\text{C}$  and  $800^\circ\text{C}$  where both temperatures are able to form the single phase with higher crystallinity of CCMO.

By observing closely to the result obtained in Fig. 2, the difference of dwelling time during sintering process gives a significant influence to phase formation of CCMO ceramic. The increasing of dwelling time favors the densification of the sample that proved by the formation of narrow and sharp peaks in the diffraction patterns. As seen from the XRD pattern, there is little decomposition of some CCMO phase occurred by the increasing the soaking sintering time. We can see that the decomposition of certain phase of CCMO

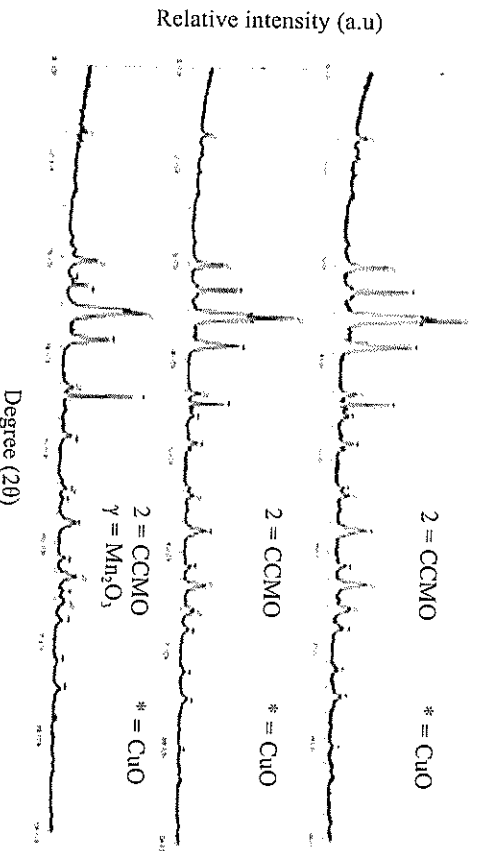


Fig. 1: XRD pattern of CCMO ceramics after being sintered for 18h at 600, 700 and 800 °C

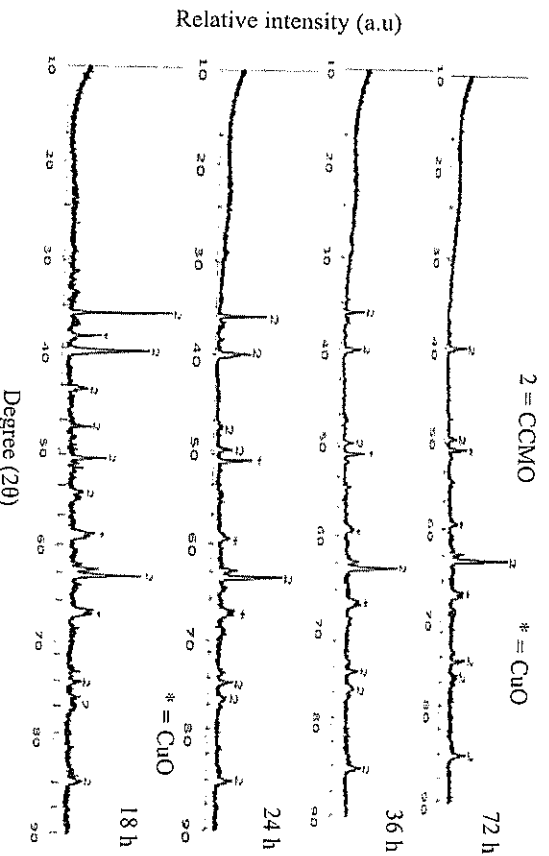


Fig. 2: XRD pattern of CCMO after being sintered at varying soaking time for 700 °C

at angle  $43.28^\circ$ ,  $47.42^\circ$  and  $54.01^\circ$  upon the increasing of soaking time.

In general, it needs about  $700^\circ\text{C}$  and 3 days under 0.18kbar (2600Psi) in order to synthesis the CCMO ceramic [5], therefore, XRD results suggested that the synthesis temperature of CCMO ceramic can be remarkably reduce from 3 days to 18 hours by sol gel synthesis without the combination of high oxygen pressure method.

#### Microstructure Characterization of CCMO Ceramic

The microstructure of the CCMO ceramics prepared from the various sintering temperature and dwelling time was presented in Figure 3 and 4. Based on the microstructure observation, the CCMO obtained from the sol gel method under atmospheric sintering condition present a mixture of plate-like grains and rod-like grains.

These suggest that the sample processing has a significant influence on the structural resulting in the different morphology of grains formation.

The FESEM micrograph results show that the lowest sintering temperature at 600°C is unable to produce better grains formation where some of coarsening grain is observed. A more uniform and homogenous grain size distribution is present by the sample sintered at 700°C for 18h. The increasing of the sintering temperature from 600°C to 800°C promotes the grain growth in the microstructure and the needles-like phase of grains particles are also clearly visible when the sample sintered up between 700°C and 800°C. By comparing the morphology results, the samples sintered at 700°C give better grains distribution, homogeneous and have more compact arrangement in grain structure compare to the result of 600°C and 800°C. These uniformity of grain formation will promotes the microstructure densification that will benefit in conduction of electrical carriers and responsible for improvements of conductivity properties. With the increasing of sintering temperature, the grain size and mechanical connection between grains are also expected to play an important role in electronic conduction [7].

*Fig. 4* is the FESEM micrograph of CCMO ceramic sintered at various soaking time. It can be observed that further increasing of dwelling time in sintering process were leads to the grain growing of microstructure. The highest of time required during sintering (72h) caused the melting features, which was adverse to the packing process between grains. Based on the results obtained, it can be concluded that the optimum (lowest) sintering parameter is at 700°C for 18h because of its capability in order to produce the better spinel morphology compared to otherparameter.

#### Magnetic Properties of CCMO Ceramic

The hysteresis loops in *Fig. 5* depict the real traces of the magnetic behavior for sintered specimen at various temperatures in 18h dwelling time. The variation data of magnetization with magnetic field (H) was collected at room temperature. By referring to the hysteresis loops, M-H curve for all sample tested are linear with the field and have a small value of coercivity. The hysteresis curves are similar and can be identified as a soft magnet by having a higher value in saturation magnetization ( $M_s$ ) and coercive force ( $H_c$ ) and

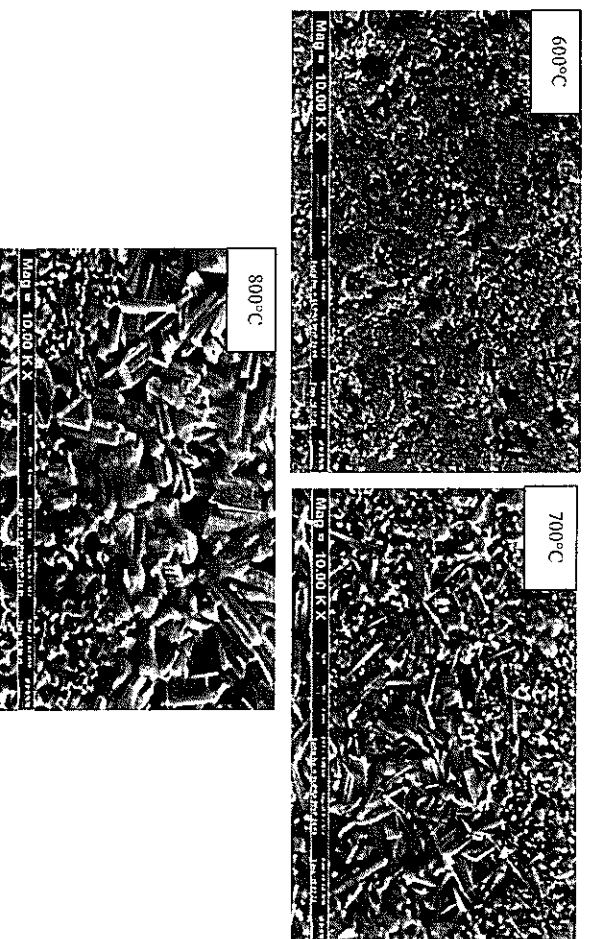


*Fig. 3. FESEM micrograph of CCMO ceramic sintered at 600 °C, 700 °C, and 800 °C for 18h*

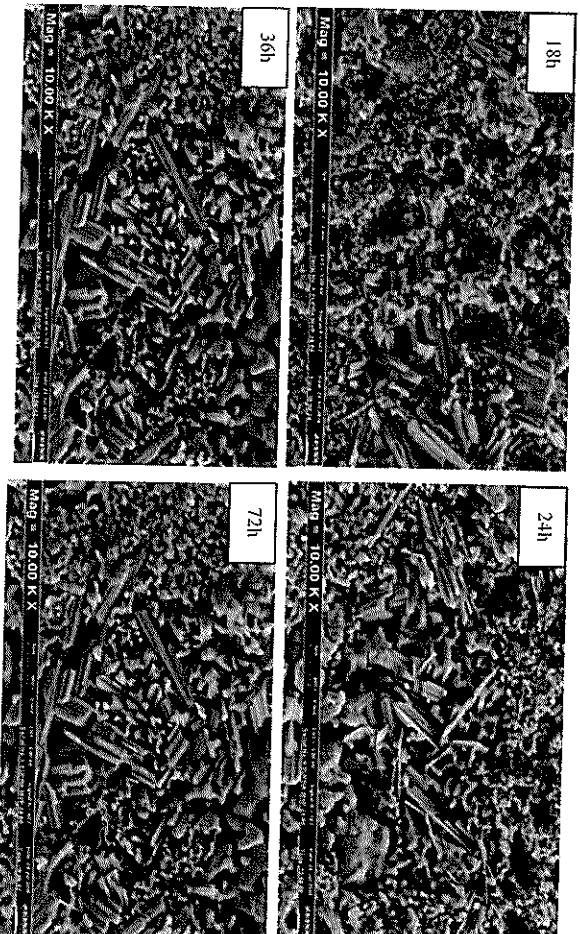


Fig. 4: FESEM micrograph showing the CCMO ceramic sintered at 18, 24, 36 and 72 h for 700 °C

have a lower value for remanence magnetization ( $M_r$ ). At room temperature, the magnetization curves for all samples show no hysteresis which indicated the “superparamagnetic” character. The highest value of  $M_r$  and  $H_c$  are 0.0128 emu  $\text{g}^{-1}$  and 235.23 Oe for sintering at 700°C, respectively which is higher than 600 and 800°C.

This differential of magnetization behavior is actually influenced by the difference of sample morphology, where the magnetic behavior is affected by the particle size [8]. As the particles are reduced, the surface/volume ratio will increase and hence the role of surface in magnetic behavior becomes more and more important [9].

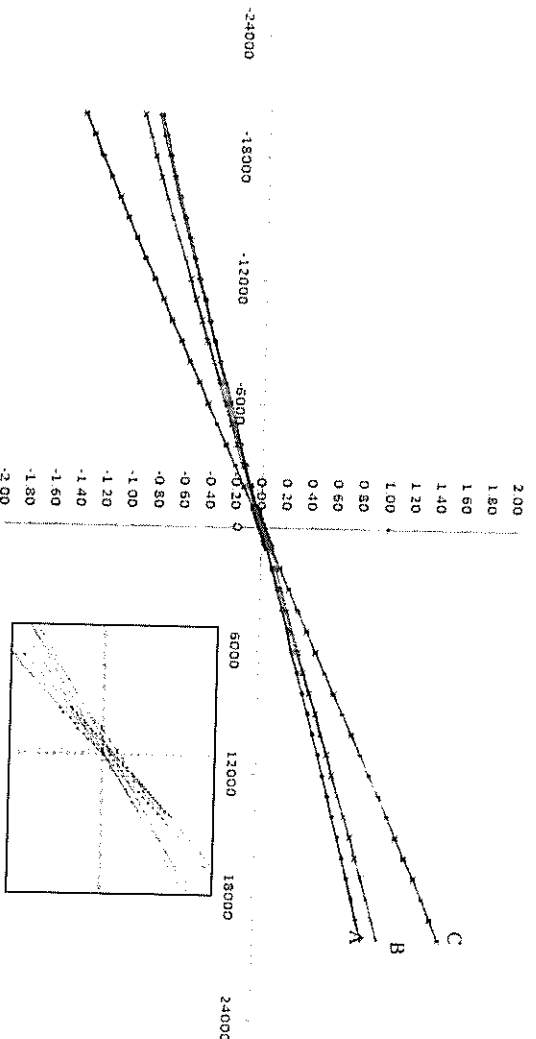


Fig.5: Room temperature  $M-H$  curves for CCMO sintered pellets at (A) 600°C; (B) 700°C and (C) 800°C.

Table 1: Magnetic characteristic of sintered CCMO sample at different temperature for 18h

| Sintering temp | M <sub>max</sub> (emu/g) | M <sub>s</sub> (emu/g) | M <sub>i</sub> (emu/g) | H <sub>c</sub> (Oe) | H <sub>s</sub> (Oe) |
|----------------|--------------------------|------------------------|------------------------|---------------------|---------------------|
| 600 °C, 18h    | 0.8363                   | 0.8363                 | 0.0051                 | 125.06              | 18932.62            |
| 700 °C, 18h    | 0.9547                   | 0.9457                 | 0.0128                 | 235.23              | 18565.43            |
| 800 °C, 18h    | 1.417                    | 1.417                  | 0.0028                 | 34.01               | 18672.45            |

The value of H<sub>c</sub> became decreasing by increasing the sintering temperature. As refer to Table 1, the lowest value of H<sub>c</sub> was obtained at 34.01 Oe for sample sintered at 800°C. This may have been due to the phenomenon of over grown magnetocrystallites that capable causing the transition from a single magnetic domain to a multi-magnetic domain structure at high temperature. Low H<sub>c</sub> value can be attributed to large grain size whereas decreasing grain size may expect increase in coercivity [10]. The H<sub>c</sub> also strongly affected by grain or particle and may reach a maximum value during the single magnetic domain or multi-magnetic domain stages of structure as reported by Albuquerque *et al.*, (2000).

## CONCLUSIONS

In this work, the CCMO electroceramic was successfully synthesized via sol gel synthesis and well densified at relative low temperature under atmospheric pressuring sintering condition. The influences of the sintering parameter on the evolution of microstructure, phase formation and magnetic properties of CCMO are also studied. The sample shows the good characteristic and promotes better properties and magnetization values at optimum lowest sintering parameter; 700 °C in 18h of dwelling time.

## ACKNOWLEDGEMENT

Thankful to Universiti Teknikal Malaysia Melaka (UTeM) for granting the research fellowship (PJP/2009/FKP (21A) S611) and gratefully acknowledged for granting access to the available research facilities.

## REFERENCES

- [1] Li, L.W., Fu, Z.Y., & Zhang, J.Y. (2006). Influence of Sintering Temperature on Microstructure and Magneto-transport Properties of La<sub>0.8</sub>Na<sub>0.2</sub>MnO<sub>3</sub> Ceramics. *Materials Letters*, **60** 970-973.
- [2] Prodi, A., Allodi, G., Gilioli, E., Licci, F., Marezio, M., Bolzoni, F., Gaurzi, A., & Derenzi, R. (2006). μSR study of AA'<sub>2</sub>Mn<sub>2</sub>O<sub>7</sub> double perovskites. *Physica B*, 55-58.
- [3] Mu, G., Yang, S., Li, J., & Gua, M. (2006). Synthesis of PZT Nanocrystalline Powder by a Modified Sol-gel Process Using Water as Primary Solvent Source. *Journal of Materials Processing Technology*, 182, 382-386.
- [4] Yang, W.D., Chang, Y.H., & Huang, S.H. (2005). Influence of Molar Ratio of Citric Acid to Metal Ions on Preparation of La<sub>0.8</sub>Sr<sub>0.3</sub>MnO<sub>3</sub> Materials via Polymerizable Complex Process. *Journal of the European Ceramic Society*, **25**, 3611-3618.
- [5] Zeng, Z., Greenblatt, m., Sunstrom IV, J.E., & Croft, M. (1999). Giant Magnetoresistance in CaCu<sub>2</sub>Mn<sub>2</sub>O<sub>7</sub>-Based Oxides with Perovskite-Type Structure. *Journal of Solid State Chemistry*, **147** 185-198.
- [6] Wu, X., Wen, Z., Xu, X., Gu, Z. & Gu, X. (2008). Optimization of a Wet Chemistry Method for Fabrication of Li<sub>2</sub>TiO<sub>3</sub>. *Journal of Nuclear Materials*, **373** 206-211.
- [7] Lei, L.W., Fu, Z.Y., & Zhang, J.Y. (2006). Influence of Sintering Temperature on Microstructure and Magneto-transport Properties of La<sub>0.8</sub>Na<sub>0.2</sub>MnO<sub>3</sub> Ceramics. *Materials Letters*, **60** 970-973.
- [8] Ozkaya, T., Baykal, A., Kavas, H., Koseoglu, Y., & Toprak, M.S. (2008). A Novel synthesis Route to Mn<sub>2</sub>O<sub>4</sub> Nanoparticles and Their Magnetic Evaluation. *Physica B*, **403** 3760-3764.
- [9] Rao, G.N., Yao, Y.D., & Chen, J.W. (2005). Supermagnetic Behavior of Antiferromagnetic

Characterization of Microstructure and Magnetic Properties of  $\text{CaCu}_2\text{Mn}_2\text{O}_7$  by Sol Gel Route

- CuO Nanoparticle. *IEEE Transaction on Magnetics*, **41** (10) 3409-3411.
- [10] Sedlar, M., Matejec, V., Grygar, T., & Kadlecova, J. (2000). Sol-gel Processing and Magnetic Properties of Nickel Zinc Ferrite Thick Films. *Ceramics International*, **26** 507-512.
- [11] Wang, X. W., Li, W., & Shi, J. (2010). Synthesis and Phase Evolution of  $\text{LiNb}_0.6\text{Ti}_{0.5}\text{O}_3$  Powder Via Sol-Gel Method. *Particulology*, **8** (5) 463-467.

fluence  
re and  
 $\text{ZnMnO}_3$   
sci, F.,  
erenzi,  
double  
2006).  
er by a  
primary  
cessing  
(2005).  
, Metal  
aterials  
trial of  
3618.  
J.E., &  
unce in  
vskite-  
ministry;  
(2008).  
rod for  
uclear  
fluence  
re and  
 $\text{ZnMnO}_3$   
glu, Y.,  
, Route  
ignetic  
2005).  
agnetic